Pakistan J. Sci. Ind. Res., Vol. 23, Nos. 3–4, June–August 1980

THEORETICAL CALCULATIONS OF TEMPERATURE-DEPENDENT ENERGY GAP, INTRINSIC CARRIER CONCENTRATIONS, FERMI LEVEL AND INDUCED CHARGE IN THE GOLD-DOPED AND NON-GOLD-DOPED SILICON

G.R. Moghal

PCSIR Laboratories, Karachi 39

(Received March 26, 1979; revised January 8, 1980)

The communication presents calculation of the total induced charge in the gold-doped and non-gold-doped silicon at various temperatures; these calculations are based on theoretical values of the stipulated variation of Fermi level with temperature and gold concentrations in gold-doped and non-gold-doped silicon which are also presented.

The plot of the experimental values of the intrinsic carrier concentration against the reciprocal of temperature (K) is compared with the one based on theoretical values. The agreement is fairly good below 300° K when the variation of the energy gap with temperature is counted.

INTRODUCTION

Electrical and optical characteristics of the bulk single crystal semiconductor are considered to be essential for the basic understanding of any semiconductor device. Therefore, these characteristics are well documentated in literature [1–5].

Gold diffusion in the semiconductor devices is of technical importance because gold acts as a life-time killer of the minority charge carriers, allowing the increase in the switching speed of the semiconductor device [1–6]. A comprehensive review on the properties of gold in the bulk silicon has been given by Bullis [10].

Recently the interest has been centred on the effects of gold at the oxidized silicon surfaces, because of the current importance of silicon planar technology. Gold introduces negative charge centres at the silicon–silicon dioxide interface when diffused from the back side of the device substrate [11–14] thus, allowing the possibility of controlling threshold voltage of MOSFETS and fabricating n-channel enhancement mode or p-channel depletion mode devices, particularly for complementary pair operation [15, 16].

Nassibian *et al.* [17], have reported that the gold energy levels in the space-charge layer of the silicon determines the shape of the MOS device charcteristics and it does not account for the large positive shift of MOS device characteristics between theory and experiment. They have also reported that at least a part of the positive shift in threshold voltage of gold doped MOSFET is due to the ionized gold acceptor levels in the depletion region, and the main part of the positive shift is due to the negatively charged gold states at the silicon–silicon dioxide interface. However, this change in gold-doped MOS device characteristics is purely due to the surface-effects of gold. Recently it has been observed [18, 19] that the negatively charged gold centres at the interface are consistent with introducing two blocks of gold acceptor states: one close to the valence based edge and the other near to the conduction band edge; which are thought to be responsible for the positive shift of gold-doped MOS device characteristics along the gate voltage axis at room temperature irrespective of the conductivity of the device substrate. But at 78°K the MOS device characteristics of the p-type gold-doped device are shifted back in the negative direction (towards the control MOS device characteristics) along the gate voltage axis and that of the n-type gold-doped device are further shifted (from the room temperature values) along the positive gate voltage axis.

However, to study these interesting surface effects of

Eg energy band gap of silicon; g spin degeneracy factor; 2 for electrons and 4 for holes; k Boltamann's constant; L_D intrinsic Debye elngth: n electron concentration; n_i intrinsic carrier concentration, N_A accepter concentration; N^- ionized acceptor concentration; N_D donor concentration; N_D^+ ionized donor concentration; N_{AU} concentration of gold atoms; N_{AU}^- concentration of ionized gold acceptor atoms; N_{AU}^+ concentration of ionized gold donor atoms; p concentration of holes; q electronic charge of the carrier; and Q_s total induced charge in silicon.

Following values are given in KT/q units: T temperature Kelvin (K), U normalized potential, U_s normalized surface potential, U_F normalized Fermi potential, U_B normalized boron acceptor potential, U_p normalized phosphorus donor potential, U_A normalized gold acceptor potential, and U_D normalized gold donor potential. Following valus are given in eV units ψ_S surface potential, ψ_F Fermi potential, ψ_B boron acceptor potential, ψ_p phosphorus donor potential, ψ_{Au} gold acceptor potential, ψ_{Au} gold donor potential, ρ total space charge density, ϵ_r permittivity of free space, and ϵ_s dielectric constant of silicon.

gold upon the MOS device characteristics, it is essential to develop a theory which takes into account the effects of gold in the bulk silicon. The surface-effects cannot be separated from the bulk effects if this is not done.

Therefore, it is the aim of this paper primarily to calculate the position of the Fermi level with temperature from 78° to 300°K for different amounts of gold concentration, and substrate impurity doping level in gold-doped and non-gold-doped silicon. The variation of the energy gap with temperature and the intrinsic carrier concentration as a function of the reciprocal of the temperature (K) is also calculated.

Finally the total induced charge versus surface potential in the gold-doped and non-gold-doped silicon for a doping level, gold concentration, and temperature have been computed. These theoretical calculations are the part and parcel for the evaluation of the theoretical gold-doped/non-gold-doped C–V curves, channel conductance and threshold voltage.

RESULTS AND DISCUSSION

Energy Gap. Macfarlane *et al.* [20] have measured the variation of the energy gap with temperature by the optical absorption measurement technique. Later Haynes *et al.* [21] measured it with recombination radiation technique.

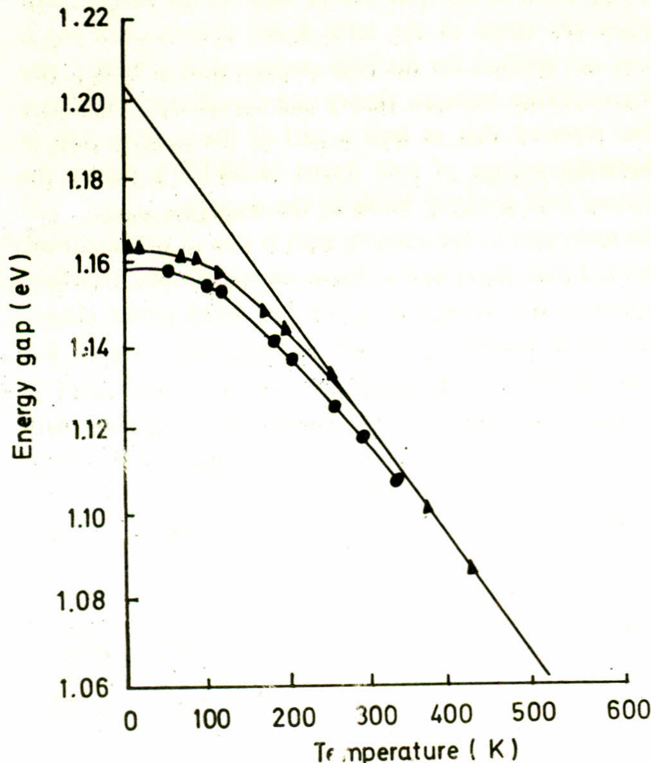

Fig. 1. Measured and computed values of the silicon energy gap as a function of temperature.: ●–● [21]; ▲–▲ [20]; computed $E_g = 1.205 - 2.8 \times 10^{-4} T$.

The former measurements indicated that transitions occurred to an exciton state 0.0073 eV below the conduction band in good agreement with the calculated exciton energy of 0.01 eV. Frova and Handler [22] measured a value of the energy gap = 1.122 eV at 296°K (when an excition energy of 0.01 eV was added) with the electro-absorption measurement technique which supported the earlier measurements. The above measurements are compared in Fig. 1. The results of Macfarlane *et al.* [20] are considered to be the most reliable because they were obtained using very high resolution (≈ 0.0015 eV) equipment, they fall near the average of the other measurements.

Intrinsic Carrier Concentration. The intrinsic carrier concentration has been measured accurately by Morin and Maita [4] with the Hall-effect and the conductivity measurements. Later Herlet [23] reported the measurements of n_i using the forward characteristics of p–n junction.

In 1958, Putley and Mitchell [24] reported the measurements of Hall-effect and the conductivity on very pure (≈ 10^{13} cm^{-3}) oxygen-free silicon. The values of n_i obtained are plotted alongwith those reported by Morin and Maita [4] and by Herlet [23] in Fig. 2, fitted with the calculated values. The values of n_i are calcuated from the following equation:

$$n_i = 3.88 \times 10^{16}\, T^{3/2} \exp\left(-\frac{E_g}{2kT}\right) \tag{1}$$

If n_i is calculated from equation (1) assuming E_g varying with temperature, the experimentally measured and the computed values seem to be coincidental fairly well below room temperature. But above room temperature the computed values start deviating from the measured values and if n_i is calculated from the equation:

$$n_i = 3.88 \times 10^{16}\, T^{3/2} \exp(-.605/kT) \tag{2}$$

above room temperature (300°K), the measured and the computed values are fairly close to each other. Fig. 2 shows the calculated values of n_i between 700 –230°K.

Calculations of Fermi Level in Gold-Doped and Non-Gold-Doped Silicon. The position of the Fermi level in the band gap of gold-doped and non-gold-doped silicon for any amount of gold concentrations in the bulk, and substrate impurity doping level as a function of temperature can be obtained from the solution of the charge neutrality equation in the bulk, where the band bending $\psi = 0$. The charge neutrality equation for gold-doped silicon:

$$p + N_D^+ + N_{Au}^+ = n + N_A^- + N_{Au}^- \tag{3}$$

for non-gold-doped silicon, put N_{Au}^+ and $N_{Au}^- = 0$

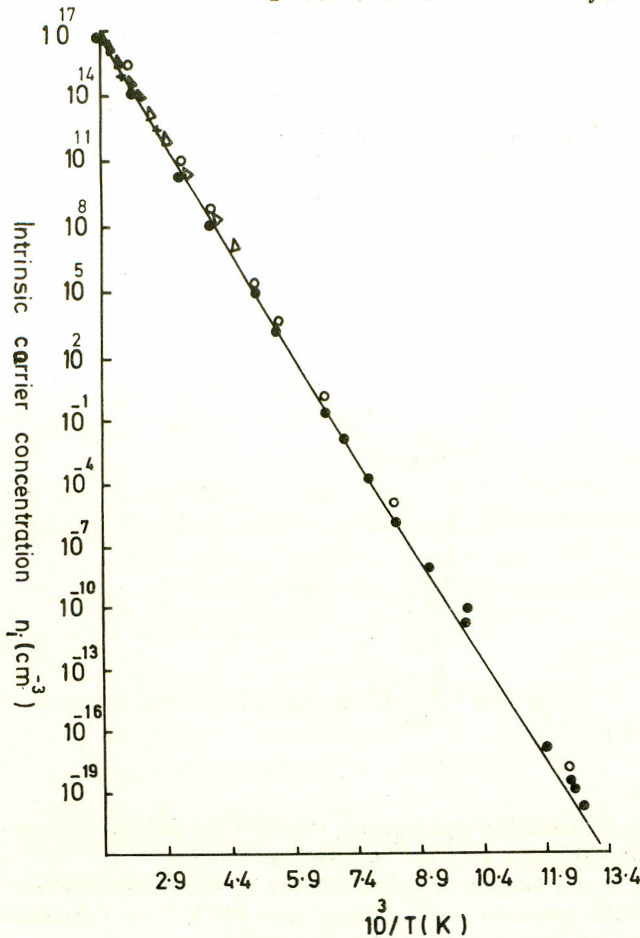

Fig. 2. Intrinsic carrier concentration in silicon between 78° and 700°K calculated and compared to experimental measurements: ▲ [4]; △ [23,24]. Present computed values with E_g varying with temperature and O: Present computed values with E_g = 121. eV. The straight line has been drawn through the solid circles using least square fit.

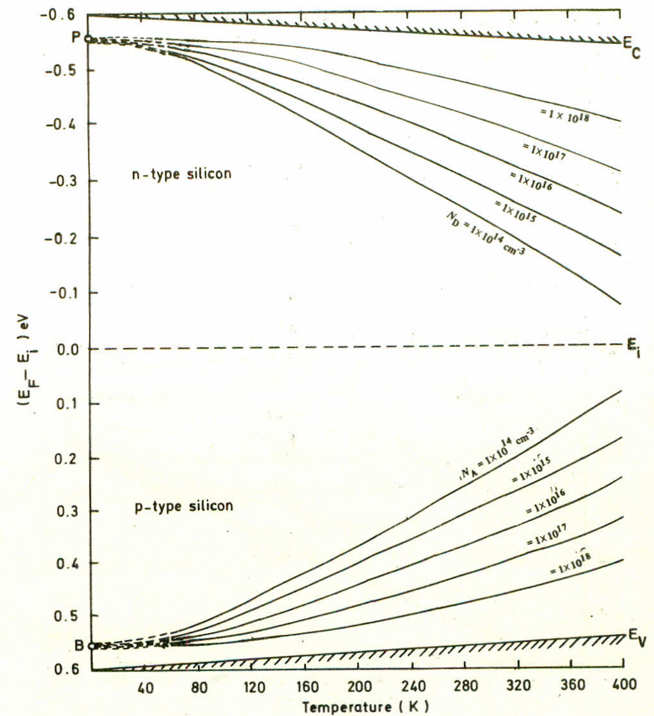

Fig. 3. The Fermi level in non-gold-doped silicon as a function of temperature, for various impurity concentrations.

where $p = n_i \exp \frac{q}{kT} \psi_F$

$$n = n_i \exp - \frac{q}{kT} \psi_F$$

$$N_D^+ = \frac{N_D}{1 + g \exp \frac{q}{kT} (\psi p - \psi_F)}$$

$$N_A^- = \frac{N_A}{1 + 1/g \exp \frac{q}{kT} (\psi_F - \psi_B)}$$

$$N_{Au}^+ = \frac{N_{Au}}{1 + 2 \exp \frac{q}{kT} (\psi_{Au}^+ - \psi_F) \left[1 + \frac{1}{2} \exp \frac{q}{kT} (\psi_{Au}^- - \psi_F)\right]}$$

$$N_{Au}^- = \frac{N_{Au}}{1 + 2 \exp \frac{q}{kT} (\psi_F^- - \psi_{Au}^-) \left[1 + \frac{1}{2} \exp \frac{q}{kT} (\psi_F - \psi_{Au}^+)\right]}$$

The equality (3) can be solved by iteration to obtain the position of the Fermi level ψ_F in the band gap of silicon for any doping level, gold concentration, and temperature Fig. 3 shows the variation of the Fermi level as a function of temperature, with doping level as a parameter in the p- and n-type non-gold-doped silicon.

Gold doping moves the Fermi level in silicon towards the position midway between the gold acceptor and donor energy levels, which are situated at 0.54 eV below the conduction band edge and 0.35 eV above the valence band edge respectively [25]. In other words gold can compensate both p- and n-type silicon but not by equal amounts because the energy levels are deep lying in the silicon [25]. However, when concentration of gold in silicon is about three orders of magnitude greater than the shallow impurity doping, the Fermi level occupies the position midway between the two gold energy levels. Fig. 4 shows the variation of the Fermi level ψ_F as a function of temperature for some known amounts of gold concentration in a substrate impurity doping level of p- and n-type gold-doped silicon. The variations of the energy band gap with temperature is also incorporated in these Figures.

Calculation of the Total Induced Charge in Gold-Doped and Non-Gold-Doped Silicon. The total charge Q_S, induced in the silicon can be evaluated by [26]:

$$Q_S = \int_{x=0}^{x=\infty} \varphi(x) dx \tag{4}$$

where x=0 corresponds to the oxide–silicon interface. The

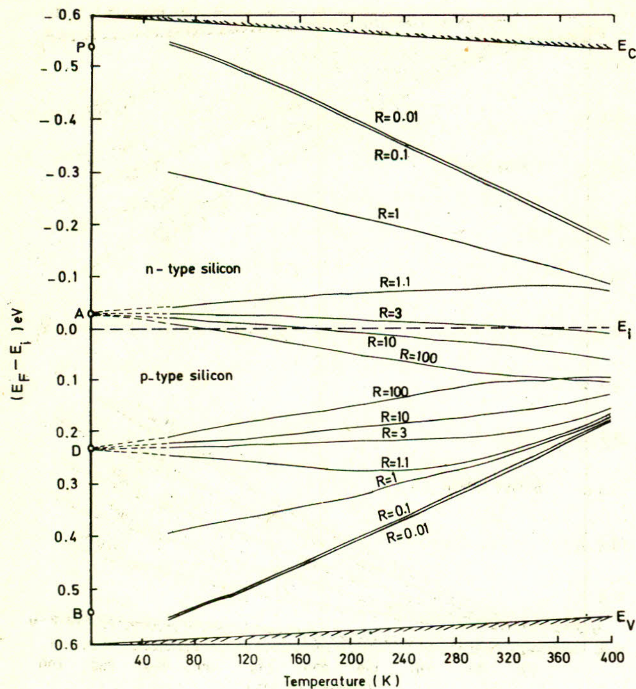

Fig. 4. The Fermi level in gold-doped silicon as a function of temperature, for various gold concentrations in a substrate doping level 1×10^{15} cm^{-3} $\left(R = \frac{\text{Gold concn}}{\text{Substrate doping level}}\right)$

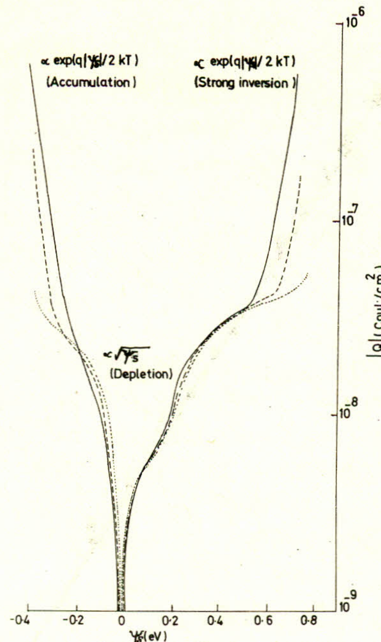

Fig. 5 Variation of total charge Q_s induced in the gold-doped p-type silicon ($N_A = 1 \times 10^{15}$ cm^{-3} and gold concentration $= 1 \times 10^{16}$ cm^{-3}) as a function of surface potential ψ_s with temperature as a variable parameter: ——— (straight line) 300°K; – – – (broken line) 200°K; and - - - - - - - (dotted line) 100°K.

charge density in the gold-doped silicon can be given by:

$$\rho' = q(p - n + N_D^+ - N_A^- + N_{Au}^+ - N_{Au}^-) \tag{5}$$

for non-gold-doped silicon put $(N_{Au}^+ - N_{Au}^-) = 0$

Assuming the silicon is non-degenerate, the total net charge within the silicon, Q_s, is obtained by substituting equation (5) in Poisson's equation:

$$\frac{d^2U}{dx^2} = \frac{-q\rho}{kT\, t_s t_r} \tag{6}$$

and integrating once one obtains:

$$Q_s = \mp \frac{U_s}{|U_s|} \; t_s t_r \frac{kT}{qL_D} \Big[\exp(U_F - U_s) - \exp(U_F) + \exp(U_s - U_F) - \exp(-U_F) - \frac{N_D}{n_i} \ln \left(\frac{g_{exp}(U_p - U_F + U_s)}{1 + g_{exp}(U_p - U_F + U_s)} \times \frac{1 + g_{exp}(U_p - U_F)}{g_{exp}(U_p - U_F)} \right) - \frac{N_A}{n_i} \ln \left(\frac{\exp(U_F - U_B - U_s)}{g + \exp(U_F - U_B - U_s)} \times \frac{g + \exp(U_F - U_B)}{\exp(U_F - U_B)} \right) + \frac{N_{Au}}{n_i} \ln \left(\frac{2 + \exp(U_F - U_D - U_s) + \exp(U_A - U_F - U_s)}{2 + \exp(U_F - U_D) + \exp(U_A - U_F)} \right) \Big]^{1/2} \tag{7}$$

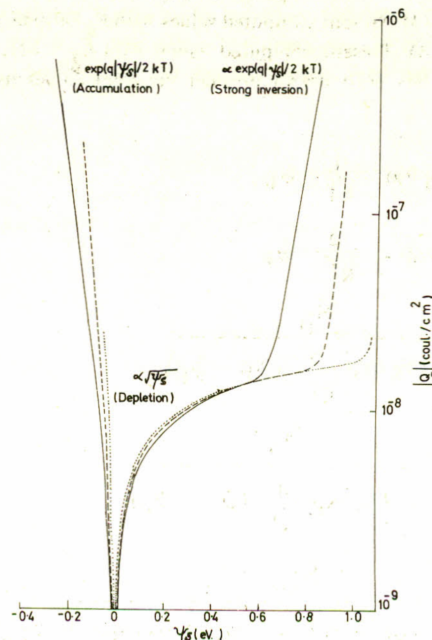

Fig. 6. Variation of total charge Q_s induced in the non-gold-doped p-type silicon ($N_A = 1 \times 10^{15}$ cm^{-3}) as a function of surface potential ψ_s, with temperature as a variable parameter: ——— (straight line): 300°K, – – – (broken line) 200°K; and - - - - - (dotted line) 100°K.

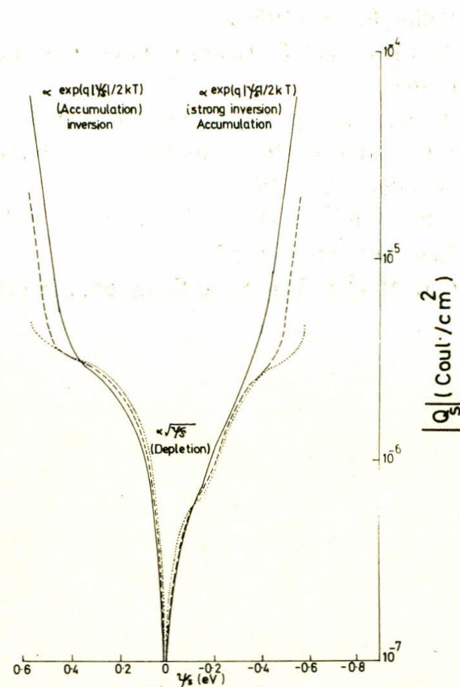

Fig. 7. Variation of total charge Q_s, induced in the gold-doped n-type silicon ($N_D=1 \times 10^{16}$ cm^{-3}) and gold concentration 1×10^{16} cm^{-3} as a function of surface potential ψ_s, with temperature as a variable parameter: —— (straight line) 300°K; – – – (broken line) 200°K, and - - - - - (dotted line) 100°K.

The equation (7) was evaluated from the accumulation to the inversion, heavy band bendings. The variation of the total induced charge with surface potential (Q_s/ψ_s) in the gold-doped and non-gold-doped p- and n-type silicon can be seen from Figs. 5–8, respectively.

Conclusion

The energy bandgap decreases with increasing temperature and the temperature coefficient $\frac{\partial Eg}{\partial T}$ is found to be -2.4×10^4 for silicon.

The values of n_i below 300°K obtained from the equation 1, assuming, E_g variable with temperature follows fairly the extrapolated part of the experimentally measured n_i vs $\frac{1}{T}$ plot and seems to be accurate.

When the Fermi level lies above the gold acceptor level most of the gold atoms are negatively charged. But when the Fermi level is between the two gold levels most of the gold atoms are neutral, and when the Fermi level is below the donor level most of the gold atmos are positively charged.

The Q_s/ψ_s relationship can be approximated into three separate forms corresponding to the regions of accumulation, depletion and inversion. The charge in the accumulation and inversion regions is exponentially varying with surface potential, and in the depletion region, it is

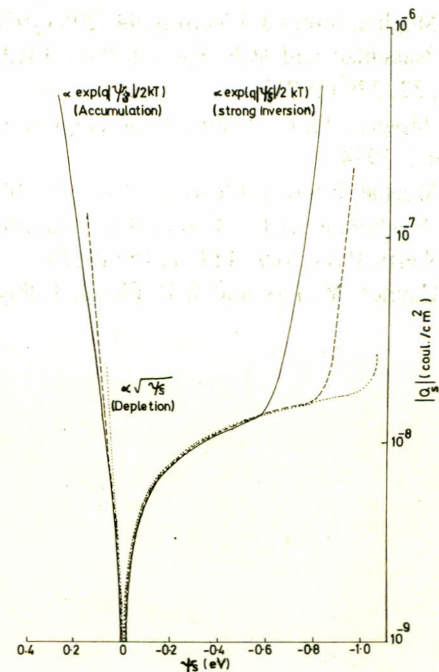

Fig. 8. Variation of total charge Q_s, induced in the non-gold-doped n-type silicon ($N_D=1 \times 10^{15}$ cm^{-3}) as a function of surface potential ψ_s, with temperature as a variable parameter: —— (straight line) 300°K; – – – (broken line) 200°K; and - - - - - (dotted line) 100°K.

parabolically varying with surface potential.

Acknowledgement. Thanks are due to Mr. S. Wajahat Ali for a critical reading of the original manuscript.

REFERENCES

1. G.L. Pearson and J. Bardeen, Phys. Rev., **75**, 865 (1949).
2. H.B. Briggs, Phys. Rev., **77**, 287 (1950).
3. E.M. Conwell, Proc. I.R.E., **40**, 1327 (1952).
4. F.J. Morin and J.P. Maita, Phys. Rev., **96**, 28 (1954).
5. S.M. SZE, *Physics of Semiconductor Devices* (Wiley, London, 1969), p. 51.
6. G.K. Wertheim and W.M. Augustyniak, Rev. Sci. Instrum., **27**, 1062 (1956).
7. G. Bemski, Phys. Rev., **111**, 1515 (1958).
8. M. Ishigame, Japan J. Appl. Phys., **3**, 720 (1964).
9. J.M. Fairfield and B.V. Gokhale, Solid State Electron., **8**, 685 (1965).
10. W.M. Bullis, Solid State Electron., **8**, 189 (1965).
11. A.G. Nassibian (a) Solid State Electron., **10**, 879 (1967); (b) *ibid*, **10**, 891 (1967).
12. S.F. Cagnina and E.H. Snow, J. Electrochem. Soc., **114**, 1165 (1967).
13. S.D. Brotherton, J. Appl. Phys., **42**, 2085 (1927).
14. D.R. Lamb, G.R. Moghal and Hawkins, Intern J. Electron., **30**, 141 (1971).
15. P. Richman, Proc. I.E.E.E., **56**, 774 (1968).

16. G.R. Moghal, Intern.J. Electron.,**44**, 205 (1978).
17. A.G. Nassibian and M.E. Sproull, Proc. I.R.E.E., Australia, **32**, 239 (1971).
18. G.R. Moghal, Ph.D. Thesis, Southampton University England, 1974.
19. G.R. Moghal, Intern.J. Electron., **46**, 313 (1979).
20. G.G. Macfarlane, T.P. Mclean, J.E. Quarrington and V. Roberts, Phys. Rev., **111**, 1245 (1958).
21. J.R. Haynes, M. Lax and W.F. Flood, J. Phys. Chem. Solids, **8**, 392 (1959).
22. A. Frova and P. Handler, Phys. Rev. Lett., **14**, 178 (1965).
23. A. Herlet and Z. Angew, Phys. Rev., **9**, 155 (1957).
24. E.H. Putley and W.H. Mitchell, Proc. Phys. Soc. (London), **A72**, 193 (1958).
25. C.B. Colling, R.O. Carlson and C.J. Gallagher, Phys. Rev., **105**, 1168 (1957).
26. G.R. Moghal, Thin Solid Films, **55**, 329 (1978).